Two-step fabrication of R-$PbI_{4(1-y)}Br_{4y}$ type light emitting inorganic-organic hybrid photonic structures

Shahab Ahmad and G. Vijaya Prakash*

Nanophotonics lab, Department of Physics, Indian Institute of Technology Delhi, New Delhi-110016, India
**prakash@physics.iitd.ac.in*

Abstract: An easy fabrication approach for highly *c*-axis oriented Inorganic-Organic (IO) mixed hybrid semiconductor thin films has been demonstrated for the first time. A simple vacuum deposition technique followed by chemical processing is utilized to fabricate controlled thin films of wide range of selective compositions from R-$PbI_{4(1-y)}Br_{4y}$ (R = organic; y = 0 to 1) type IO hybrids. These thin films are alternative stack of inorganic and organic nanoscale layers, resembles multiple quantum wells. As a result, they show several novel features including tunable strong room-temperature excitons over a broad spectral range from 380 nm to 520 nm. Structural and *in situ* optical studies confirm that the methodology can be directly adoptable in top-down technology and also extendable for many varieties of inorganic-organic frameworks. The device quality fabrication process and optoelectronic multi-functionality has been demonstrated by template based 3D microstructures, exciton PL imaging and photodetector response.

OCIS codes: (160.4670) Optical materials; (250.4745) Optical processing devices; (250.5230) Photoluminescence; (160.6000) Semiconductor materials; (310.6860) Thin films, optical properties; (310.3840) Materials and process characterization.

References and links

1. C. R. Kagan, D. B. Mitzi, and C. D. Dimitrakopoulos, "Organic-inorganic hybrid materials as semiconducting channels in thin-film field-effect transistors," Science **286**(5441), 945–947 (1999).
2. D. B. Mitzi, S. Wang, C. A. Feild, C. A. Chess, and A. M. Guloy, "Conducting layered organic-inorganic halides containing (110)-oriented perovskite sheets," Science **267**(5203), 1473–1476 (1995).
3. T. Ishihara, J. Takahashi, and T. Goto, "Optical Properties Due to Electronics Transitions in Two-Dimensional Semiconductors ($C_nH_{2n+1}NH_3)_2PbI_4$," Phys. Rev. B **42**(17), 11099–11107 (1990).
4. M. Shimizu, J. Fujisawa, and J. Ishi-Hayase, "Influence of dielectric confinement on excitonic nonlinearity in inorganic-organic layered semiconductors," Phys. Rev. B **71**(20), 205306 (2005).
5. D. B. Mitzi, K. Chondroudis, and C. R. Kagan, "Organic–inorganic electronics," IBM J. Res. Develop. **45**(1), 29–45 (2001).
6. Z. Xu, D. B. Mitzi, C. D. Dimitrakopoulos, and K. R. Maxcy, "Semiconducting perovskites (2-$XC_6H_4C_2H_4NH_3)_2SnI_4$ (X = F, Cl, Br): Steric interaction between the organic and inorganic layers," Inorg. Chem. **42**(6), 2031–2039 (2003).
7. M. Era, S. Morimoto, T. Tsutsui, and S. Saito, "Organic-inorganic heterostructure electroluminescent device using a layered perovskite semiconductor $(C_6H_5C_2H_4NH_3)_2PbI_4$," Appl. Phys. Lett. **65**(6), 676–678 (1994).
8. K. Pradeesh, J. J. Baumberg and G. Vijaya Prakash, "Strong exciton-photon coupling in inorganic-organic multiple quantum wells embedded low-Q microcavity," Opt. Express **17**, 22171– 22178 (2009).
9. Z. Xu and D. B. Mitzi, "$[CH_3(CH_2)_{11}NH_3]SnI_3$: A hybrid semiconductor with MoO_3-type Tin(II) iodide layers," Inorg. Chem. **42**(21), 6589–6591 (2003).
10. N. Kitazawa, M. Aono, and Y. Watanabe, "Excitons in organic–inorganic hybrid compounds $(C_nH_{2n+1}NH_3)_2PbBr_4$ (n = 4, 5, 7, and 12)," Thin Solid Films **518**(12), 3199–3203 (2010).
11. J. Calabrese, N. L. Jones, R. L. Harlow, N. Herron, D. L. Thorn, and Y. Wang, "Preparation and characterization of layered lead halide compounds," J. Am. Chem. Soc. **113**(6), 2328–2330 (1991).
12. S. Ahmad, J. J. Baumberg and G. Vijaya Prakash, "Structural tunability and switchable exciton emission in mixed inorganic-organic hybrids," (in preparation).
13. N. Kitazawa, K. Enomoto, M. Aono, and Y. Watanabe, "Optical Properties of $(C_6H_5C_2H_4NH_3)_2PbI_{4-x}Br_x$ (x =0–4) mixed-crystal doped PMMA films," J. Mater. Sci. **39**(2), 749–751 (2004).

#196165 - $15.00 USD Received 22 Aug 2013; revised 3 Nov 2013; accepted 6 Nov 2013; published 16 Dec 2013

14. K. Pradeesh, J. J. Baumberg, and G. Vijaya Prakash, "In situ intercalation strategies for device-quality hybrid inorganic-organic self-assembled quantum wells," Appl. Phys. Lett. **95**(3), 033309 (2009).
15. T. Matsui, A. Yamaguchi, Y. Takeoka, M. Rikukawa, and K. Sanui, "Fabrication of two-dimensional layered perovskite $[NH_3(CH_2)_{12}NH_3]PbX_4$ thin films using a self-assembly method," Chem. Commun. (Camb.) **10**(10), 1094–1095 (2002).
16. T. Matsushima, K. Fujita, and T. Tsutsui, "High field-effect hole mobility in organic-inorganic hybrid thin films prepared by vacuum vapor deposition technique," Jpn. J. Appl. Phys. **43**(No. 9A/B), L1199–L1201 (2004).
17. K. Ikegami, "Spectroscopic study of J aggregates of amphiphilic merocyanine dyes formed in their pure Langmuir films," J. Chem. Phys. **121**, 2337–2341 (2004).
18. D. B. Mitzi, M. T. Prikas, and K. Chondroudis, "Thin film deposition of organic-inorganic hybrid materials using a single source thermal ablation technique," Chem. Mater. **11**(3), 542–544 (1999).
19. Z. Y. Cheng, H. F. Wang, Z. W. Quan, C. K. Lin, J. Lin, and Y. C. Han, "Layered organic-inorganic perovskite-type hybrid materials fabricated by spray pyrolysis route," J. Cryst. Growth **285**(3), 352–357 (2005).
20. D. B. Mitzi, D. R. Medeiros, and P. W. DeHaven, "Low temperature melt processing of organic-inorganic hybrid films," Chem. Mater. **14**(7), 2839–2841 (2002).
21. V. K. Dwivedi, J. Baumberg, and G. Vijaya Prakash, "Direct deposition of inorganic-organic hybrid semiconductors and their template-assisted microstructures," Mater. Chem. Phys. **137**(3), 941–946 (2013).
22. J. Takeda, T. Tayu, S. Saito, and S. Kurita, "Exciton-phonon interaction and potential fluctuation effect in $PbI_{2(1-x)}Br_{2x}$ mixed crystals," J. Phys. Soc. Jpn. **60**(11), 3874–3881 (1991).
23. H. Abid, A. Samet, T. Dammak, A. Mlayah, E. K. Hlil, and Y. Abid, "Electronic structure calculations and optical properties of a new organic–inorganic luminescent perovskite: $(C_9H_{19}NH_3)2PbI_2Br_2$," J. Lumin. **131**(8), 1753–1757 (2011).
24. Y. Kawabata, F. M. Yoshizawa, Y. Takeoka, and M. Rikukawa, "Relationship between structure and optoelectrical properties of organic–inorganic hybrid materials containing fullerene derivatives," Synth. Met. **159**(9-10), 776–779 (2009).
25. I. B. Koutselas, L. Ducasse, and G. C. Papavassiliou, "Electronic properties of three- and low-dimensional semiconducting materials with Pb halide and Sn halide units," J. Phys. Condens. Matter **8**(9), 1217–1227 (1996).
26. K. Pradeesh, J. J. Baumberg, and G. Vijaya Prakash, "Exciton switching and Peierls transitions in hybrid inorganic-organic self-assembled quantum wells," Appl. Phys. Lett. **95**(17), 173305 (2009).
27. K. Pradeesh, J. J. Baumberg, and G. Vijaya Prakash, "Temperature-induced exciton switching in long alkyl chain based inorganic-organic hybrids," J. Appl. Phys. **111**(1), 013511 (2012).
28. K. Pradeesh, K. Nageswara Rao, and G. Vijaya Prakash, "Synthesis, structural, thermal and optical studies of inorganic-organic hybrid semiconductors, R-PbI_4," J. Appl. Phys. **113**(8), 083523 (2013).
29. I. Koutselas, P. Bampoulis, E. Maratou, T. Evagelinou, G. Pagona, and G. C. Papavassiliou, "Some unconventional organic-inorganic hybrid low-dimensional semiconductors and related light-emitting devices," J. Phys. Chem. C **115**(17), 8475–8483 (2011).
30. Z. Y. Cheng, Z. Wang, R. B. Xing, Y. C. Han, and J. Lin, "Patterning and photoluminescent properties of perovskite-type organic/inorganic hybrid luminescent films by soft lithography," Chem. Phys. Lett. **376**(3-4), 481–486 (2003).
31. M. M. Lee, J. Teuscher, T. Miyasaka, T. N. Murakami, and H. J. Snaith, "Efficient hybrid solar cells based on meso-superstructured organometal halide perovskites," Science **338**(6107), 643–647 (2012).

1. Introduction

In the recent years inorganic-organic (IO) based hybrid materials have attracted considerable interest as an active material for various low-dimension semiconductor devices, having the advantages of individual entities. While inorganic semiconductors promise superior carrier mobility and thermal stability, organic material offers flexibility of process-ability [1, 2]. In the development of these potential materials, one of class of hybrids with new properties have emerged as *perovskite* type IO hybrids in the form of a two-dimensional (2D) structure represented by $(R\text{-}NH_3)_2MX_4$ where R is organic moiety, M is divalent metal (such as Pb^{2+}, Sn^{2+}, etc.) and X is halogen (such as I^-, Br^-, and Cl^-). These hybrids consists of alternative stacks of infinitely extended direct bandgap semiconductor monolayers (corner shared metal halide octahedral network) separated by larger bandgap organic (mono/di amino organic) moieties. Due to large dielectric mismatch and quantum size effects in these natural multiple quantum well (MQW) structures, exceptional enhancement in the binding energies of excitons in the inorganic sheets are observed. Therefore, these hybrid MQWs give rise to stable room-temperature *Mott* type exciton features, more stable than the bulk excitons [3, 4]. Hence the engineering of individual inorganic and organic entities of IO hybrid can be tailored to control and modify their electronic, optical, magnetic, and mechanical properties [5, 6]. By virtue of such unique room-temperature performances, several new hybrid optoelectronic devices have been emerged: such as IO-LEDs, IO-FETs, nonlinear optical switches, exciton-photon coupling photonic architectures etc [1,7,8].

#196165 - $15.00 USD Received 22 Aug 2013; revised 3 Nov 2013; accepted 6 Nov 2013; published 16 Dec 2013

A unique advantage is the exciton energy tuning by structural engineering of semiconducting metal halide layers. For example, the replacement of Sn^{2+} with Pb^{2+} in MI_4^{2-} inorganic network results in the variation of room-temperature exciton features from 620 nm to 510 nm [9]. Similarly, in PbX_4^{2-} network, the replacement of halide (X^-) species from I^- to Br^- to Cl^-, alter the excitons from 520 nm to 400 nm to 280 nm respectively [5–12]. Furthermore, by selective compositional replacement of either halide or metal atoms within inorganic network result into desired tunability in the exciton features [12,13]. However, such advantages can only be achieved when these hybrids are highly *c*-oriented having alternative stacks of inorganic and organic networks. This is always been a formidable task, since conventional chemical natural self-assembly process more often result differently [14].

Traditionally these IO hybrid thin films are fabricated by standard spin/dip coatings from chemically synthesized powders and crystals. Other thin film technologies are also been experimented, such as electrochemical deposition, single and dual source thermal vapor deposition, Langmuir Blodgett (LB) method, layer by layer deposition, spray pyrolysis [13–21]. However, it is always difficult to find empirical conditions and processes to obtain well-ordered thin films of these IO-hybrids [13–21]. However a suitable and direct method to fabricate device quality thin films is still a bottleneck for device fabrication, exclusively for those require 3D structures. Further, such methodologies are even more complex for mixed metal halide hybrid compositions fabricated from conventional chemical synthesis followed by spin coating [12,13]. Therefore it is very important to establish an easily processible and low-cost method for effective usage in new-generation optoelectronic devices.

In this paper, an easy approach for fabrication of device quality thin films of mixed inorganic-organic hybrids has been demonstrated. Highly crystalline and smooth films of $(RNH_3)_2PbI_{4(1-y)}Br_{4y}$: y = 0 to 1 have been fabricated by simple two - step process using intercalation strategies. Structural studies shows the smooth topography and highly crystalline nature of these strongly c-axis oriented thin films and *in situ* optical studies reveals the evolution of desired exciton features from mixed IO hybrids. The demonstrated capabilities such as 3D micropatterning, PL imaging and photodetector response reveal the potential of the developed methodology applicable for several electronic and photonic device applications.

2. Experiment

A novel intercalation strategy for fabrication of inorganic-organic hybrid device quality films has been recently developed [14]. Using this method a series of mixed IO hybrid thin films of $(R\text{-}NH_3)_2PbI_{4(1-y)}Br_{4y}$, y = 0 to 1 have been fabricated from thermal vacuum deposited inorganic films followed by simple chemical process, as shown in Fig. 1. Desired thin films of metal-halides PbI_2, $PbBr_2$ and $PbI_{1.0}Br_{1.0}$ are deposited by thermal vapor deposition (at vacuum ~10^{-6} torr). $PbI_{1.0}Br_{1.0}$ powder have been synthesized by dissolving the PbI_2 and $PbBr_2$ in Di-methylformamide (DMF) in stoichiometric amounts. In order to generalize the fabrication we have experimented different mixed IO hybrids, $(C_6H_9C_2H_4NH_3)_2PbI_{4(1-y)}Br_{4y}$ (hereafter CHPIB) and $(C_{12}H_{25}NH_3)_2PbI_{4-y}Br_{4y}$ (C12PIB). While all of them show excellent results, here we report only the results of CHPIB. For CHPIB, the organic iodide and bromides, $((C_6H_9C_2H_4NH_3)I$, $(C_6H_9C_2H_4NH_3)B$ (hereafter CHI and CHB respectively) powders have been synthesized by the method mentioned elsewhere [14]. The intercalation process has been performed for 10 sec by dipping the deposited metal halide film in the desired organic moiety solution at room-temperature. For the compositions y = 0 (CHPI) and 1.0 (CHPB) are obtained from thermal deposited PbI_2 and $PbBr_2$ films respectively. For mixed compositions (y = 0.25, y = 0.50 and y = 0.75) $PbI_{1.0}Br_{1.0}$ films are used. Figure 1 explains the intercalation strategies adopted for the fabrication of several compositions of CHPIB thin films.

#196165 - $15.00 USD Received 22 Aug 2013; revised 3 Nov 2013; accepted 6 Nov 2013; published 16 Dec 2013

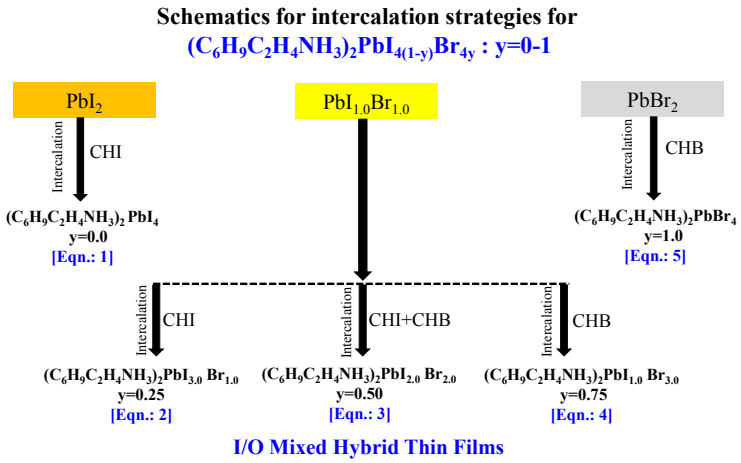

Fig. 1. Various intercalation strategies adopted for fabrication of mixed IO hybrid thin films of $(C_6H_9C_2H_4\ NH_3)_2PbI_{4(1-y)}Br_{4y}$: y = 0 to 1.

Glancing angle thin film X-Ray Diffraction studies of all as-deposited ($PbI_{1.0}Br_{1.0,}$ PbI_2 and $PbBr_2$) and processed thin films were carried out with Cu Kα radiation (λ = 1.5406 Å). The optical absorption measurements of thin films were carried out using a white light source and a spectrometer. Photoluminescence (PL) measurements were carried out on both commercial emission spectrometer as well as home built setup. The *in situ* time dependent PL and absorption measurements has been performed simultaneously using white-light source, 410 nm diode laser and a spectrometer. The PL, conventional bright field images and PL spectral line scans are performed by using a modified confocal microscope coupled with 410 nm diode laser and equipped with motorized XY stage. The SEM images of the template IO hybrid structures have been recorded using table top Hitachi SEM (Model No. TM3030). Photocurrent measurements are performed using Xe lamp source coupled to a monochromator (~109mW at 410 nm) and digital nano-ammeter and D.C. voltage source.

3. Results and discussion

The crystallinity, phase formation, structural re-arrangement and structural differences between the as-deposited metal halide (PbI_2 and $PbBr_2$, $PbI_{1.0}Br_{1.0}$) films and the resultant mixed composition IO hybrid thin films have been characterized by glancing angle X-ray diffraction technique. Figure 2(a) compares the diffraction pattern of as-deposited thin films of PbI_2, $PbBr_2$ and $PbI_{1.0}Br_{1.0}$. The X-ray diffraction patterns of PbI_2 and $PbBr_2$ shows the presence of layered type hexagonal and orthorhombic [22] phases respectively. The X-ray diffraction pattern of mixed composition $PbI_{1.0}Br_{1.0}$ shows entirely different diffractions than parental PbI_2 and $PbBr_2$, suggesting the mixed metal halide alloy, though further experiments are needed to find exact composition details.

#196165 - $15.00 USD Received 22 Aug 2013; revised 3 Nov 2013; accepted 6 Nov 2013; published 16 Dec 2013

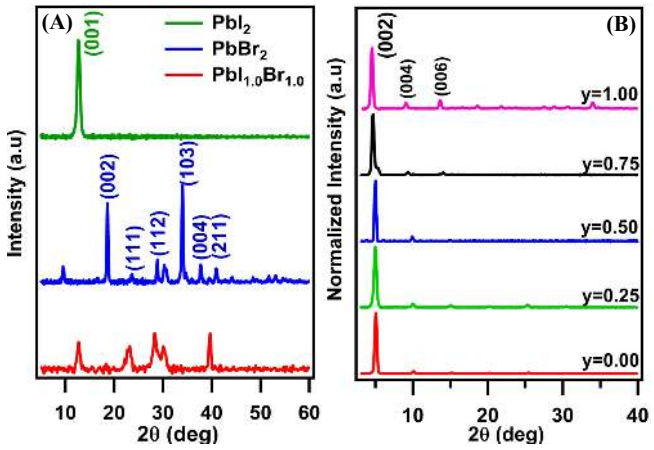

Fig. 2. (A) X-ray diffraction pattern of thermal vapor deposited thin films of PbI_2, $PbBr_2$ and $PbI_{1.0}Br_{1.0}$. (B) X-ray diffraction pattern of intercalated mixed IO hybrid thin films of $(C_6H_9C_2H_4\ NH_3)_2PbI_{4(1-y)}Br_{4y}$: y = 0 to 1.

Several compositions of CHPIB: from y = 0 to 1, using metal halide films are being fabricated from the intercalation of organic moiety (CHI or CHB or both). Figure 2(b) shows the X-ray diffraction patterns of those obtained films. Strong diffraction peaks corresponding to the *(002l)* reflection shows that all the intercalated mixed IO hybrid films are highly oriented along c-axis, perpendicular to the substrate. These characteristic XRD patterns confirm the systematic phase transformation of all polycrystalline metal-halide and mixed metal halides into highly oriented self-assembled inorganic-organic hybrid thin films. Moreover, a systematic shift in the dominant (*002l*) peak towards lower diffraction angles (accordingly d-spacing) with increasing bromine content in the PbX network has also been observed [Fig. 3].

The basic crystal packing of these $(R\text{-}NH_3)_2MX_4$($M = Pb^{2+}$, Sn^{2+} etc., and $X = I^-$, Br^- etc.) type hybrids, consists of layers of corner-shared MX_6 octahedra and bi-layers of organic cations stacked alternatively. The side-linked inorganic octahedra are extended as 2D planar sheets and the adjacent layers are coupled by organic moieties via weak hydrogen bonds through NH_3 ligands of the organic cations [5]. Therefore, these 2D systems are regarded as natural multiple quantum well (MQW) structures. The systematic change in the X-ray diffraction with addition of Br result indicates that there is a systematic transformation in the PbX_4^{2-} network, while retaining the layered arrangement. Further these intercalated mixed IO hybrid thin films show higher quality layered arrangement than the films fabricated by solution chemistry based spin coating and other traditional methods [5,12,13]

Recently it has been demonstrated that in mixed IO hybrids, Br atoms first occupy the terminal halide positions in the PbX octahedron, without distorting the layered arrangement [Fig. 3(c)] [23]. Therefore, it is convenient to predict from the present XRD results that during intercalation process the self-assembly of both, metal halide layers as well as organic moieties takes place which leads to the alternate stacking of inorganic and organic layers with a systematic replacement of large ionic radii I atoms (y = 0.0) with relatively smaller Br atoms (y = 1.0). However, such inorganic network selective substitution can be better understood after a detailed structural investigation.

#196165 - $15.00 USD Received 22 Aug 2013; revised 3 Nov 2013; accepted 6 Nov 2013; published 16 Dec 2013

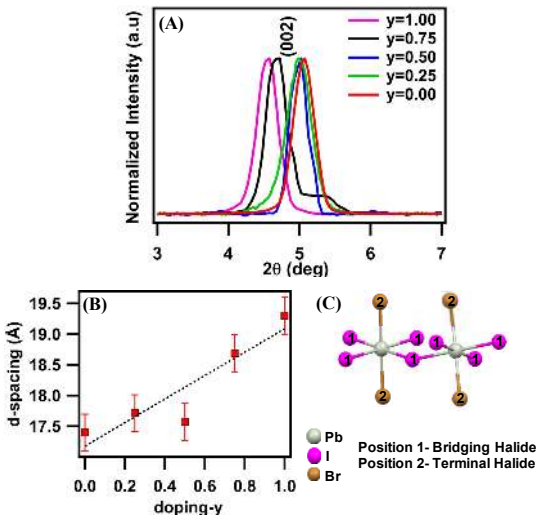

Fig. 3. (a) Shows the systematic shift in the *(002)* characteristic XRD peak (from Fig. 2) with increase in doping value *y*. (b) Shows the monotonous increment in d-spacing with increase in the Br composition in the inorganic network (C). Schematic and possible representation of inorganic network for (R- NH_3)$_2$ $PbI_{4(1-y)}Br_{4y}$ at y = 0.5 (organic is not shown here) [23].

The absorption and photoluminescence studies of intercalated mixed IO hybrid films have been performed at room-temperature [Figs. 4(a) and 4(b)]. All the films exhibit sharp (~20-30 nm line widths) and intense absorption bands between ~380 nm to 510 nm [Fig. 4(a)] Both PL and absorption sharp excitonic peaks show a systematic shift towards lower wavelength with increasing Br content (y). Similar systematic shifts from ~517 nm to 402 nm in the narrow PL is observed [Fig. 4(b)] on excitation at 337 nm wavelength.

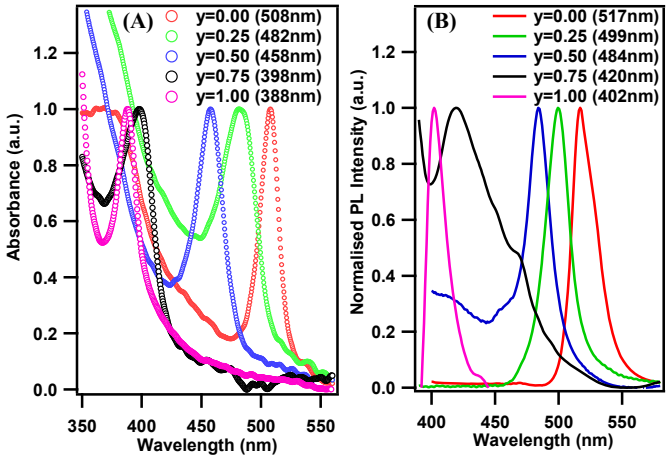

Fig. 4. Room temperature (a) UV-visible absorption and (b) Photoluminescence (λex~337 nm) spectra of the intercalated mixed IO hybrid thin films of $(C_6H_9C_2H_4NH_3)_2PbI_{4(1-y)}Br_{4y}$:y = 0 to 1.

Due to the influence of dielectric and quantum confinement effects, these layered *perovskites* exhibit sharp exciton peaks in the absorption and photoluminescence (PL) spectra at room-temperature [24]. It is generally accepted that the lowest fundamental optical transitions in $(RNH_3)_2PbX_4$ is similar to that of parent inorganic PbX_2 [3,25]. In PbX_2, the top of the valence bands is composed of Pb(6s) orbitals hybridized with X(n, p) [where n = 5 for I and n = 4 for Br] orbital and the bottom of the conduction band is essentially of Pb(6p) character. The Br(4p) orbital energy is lower than that of the I(5p) orbital, hence the optical

#196165 - $15.00 USD Received 22 Aug 2013; revised 3 Nov 2013; accepted 6 Nov 2013; published 16 Dec 2013

bandgap of Pb-Br hybrid systems are supposed to be larger than in Pb-I hybrids. In our recent works [26–28], the optical bandgap values are directly correlated to the exciton transitions. Thus it can be inferred that both exciton absorption and PL shifts toward higher energies, due to active participation of substituting Br atoms in the band structure [12,13]. While in the basic metal halide mixed semiconductors the exciton energy systematic shift with the composition is well studied, in the present mixed IO hybrids the understanding of exciton behavior requires much elaborate study and analysis, which will be reported elsewhere [12].

In order to ensure the single phase of such intercalated mixed IO hybrid films, room-temperature *in situ* experiments has been performed to monitor the evolution of desired IO hybrid from the parent inorganic thin films. For this purpose real-time PL and absorbance spectra are monitored simultaneously for two specific compositions y = 0.00 and y = 0.25 and the spectra are recorded at a time interval of 100ms. The wavelength-time PL intensity images shows a systematic smooth and consistent evaluation of single PL peak (at λ_{em} = 499 nm) for mixed IO hybrids film of composition y = 0.25 [Figs. 5(b) and 5(c)], as compared to the obvious results obtained for y = 0.00 (at λ_{em} = 517 nm) [Fig. 5(a)]. These real time *in situ* experiments confirm the authenticity of the proposed method to develop device quality IO hybrid thin films of having compositional dependent optical excitons. The exciton absorption and PL peak intensities for both compositions are plotted in Fig. 5(d) and 5(e) respectively. In general the exciton absorption is an average effect from all exciton levels, whereas the PL is only from the lowest available exciton energy levels. The exciton absorption evaluation follows double exponential behavior independent of inorganic composition [14]. For both samples, the absorption peak intensity vs intercalation time curve is showing a quick initial rise producing attenuation of up to 40-60%. This is followed by a slower rise in the exciton phase built-up which ends up showing saturation of exciton absorption. For composition y = 0.25, the absorption initial rise reaches to saturation just below 5 seconds, whereas in y = 0.00 it is upto 46 seconds. In both the cases, the intercalation is complete within 50sec duration with expected single phase evolution. But in the case of PL time evolution [Fig. 5(e)], for y = 0.00 compound the PL peak intensity reaches to a saturation at about 50 seconds followed by slow decay. In general, the exciton features in these IO hybrids are strongly dependent on the several key factors, such as structural reorganization of inorganic network, the size and shape of intercalating organic moiety and the solvent that is used for intercalation. Therefore, a detailed study of dynamic evolution of intercalation process requires a special attention to address fully the influencing factors, which will be our future directive.

#196165 - $15.00 USD Received 22 Aug 2013; revised 3 Nov 2013; accepted 6 Nov 2013; published 16 Dec 2013

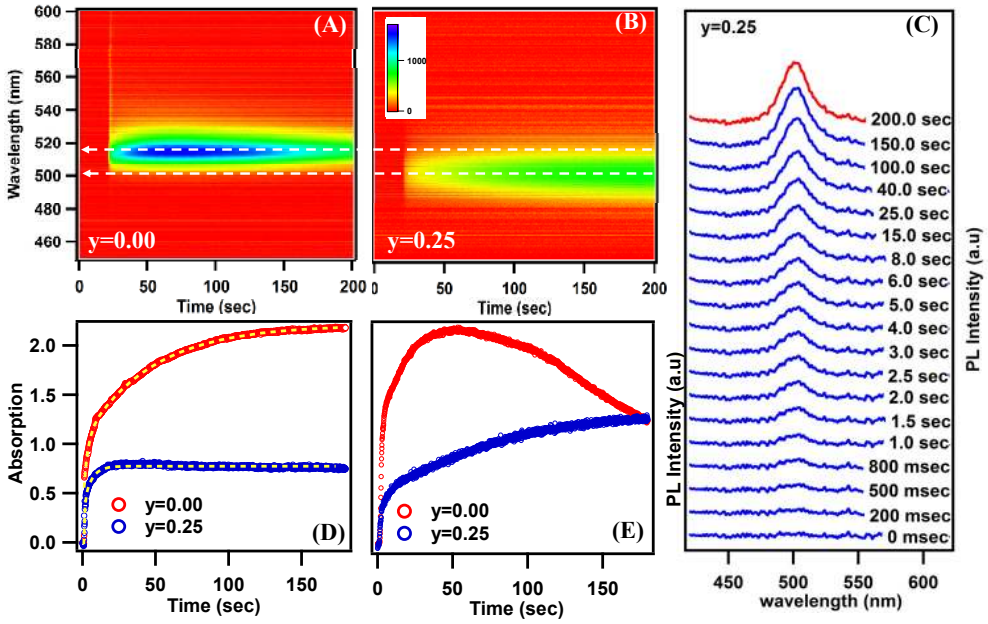

Fig. 5. PL spectral-time intensity images for real time monitoring the evolution of excitons PL from mixed IO hybrid $(C_6H_9C_2H_4NH_3)_2PbI_{4(1-y)}Br_{4y}$ for the compositions (a) y = 0.00 and (b) y = 0.25 respectively. (c) excitonic-PL spectral phase evaluation for composition y = 0.25 (same as Fig. 5(b)). Exciton (d) absorption and (e) PL peak intensities vs time plots extracted from *in situ* measurements monitored for y = 0.00 and y = 0.25 composition films respectively. Dotted lines in Fig. 5(d) are double exponential fits.

For practical applications, such as mixed IO hybrid thin films are to be carved into sub-microscale photonic/electronic devices like LED or photodetectors/sensors [7,8,29]. Therefore it is essential to establish the suitability of this thin film technology for potential use in fabrication, compatible with lithographic techniques [30] and ion/laser beam writings. The flexibility of making desired patterns or structures, which was not possible earlier with the conventional methods, is hereby demonstrated. As an example, sub-micron size circular (~670μm) structures are used as templates to create $PbI_{1.0}Br_{1.0}$ micron structures (about ~50 nm thick) through thermal vapor deposition. These patterned structures are processed to obtain mixed IO hybrid structures of CHPIB: y = 0.25, using the optimized procedure mentioned before. Scanning electron microscope (SEM) images shows the uniformity of the structures [Fig. 6(a)]. The surface quality of the structures before and after chemical processing is also been ensured by Atomic force microscopy (not shown here) where the average roughness is found to be less than 4 nm. Confocal PL images [Fig. 6(b)] confirms the strong and uniform luminescence from these template structures, as visible to naked eye. . However, recently we have demonstrated that the optical exciton energies are strongly dependent on the structural deformation, crystal defects and thickness [8,14,26]. In view of this, the PL spectral line scans are performed on microstructures by focusing the low-power excitation laser down to ~40μm spot size and collected the spectra at the image plane (size 3.5x2.7mm^2) at 50μm area. The PL spectral line scan intensity image has been reproduced in Fig. 6(c). The PL peak maxima and corresponding PL intensity over the scanned length has been plotted separately in Fig. 6(d).

#196165 - $15.00 USD Received 22 Aug 2013; revised 3 Nov 2013; accepted 6 Nov 2013; published 16 Dec 2013

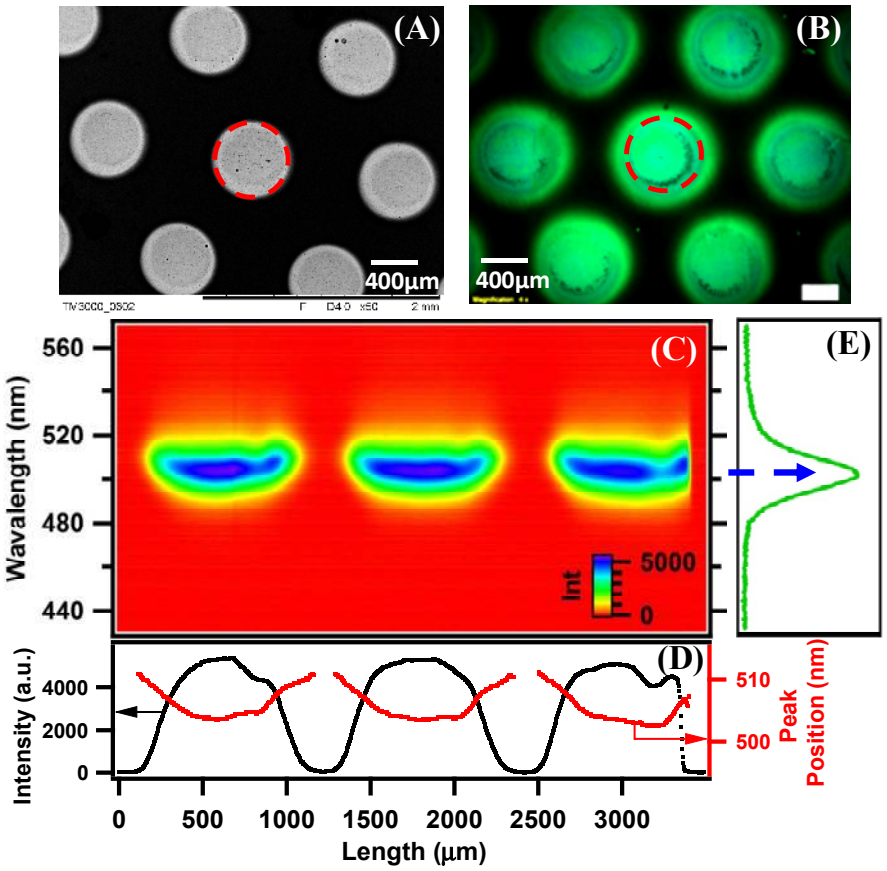

Fig. 6. (a) SEM images of patterned structures of mixed IO hybrids at y = 0.25 deposited on glass substrate. (b) and (c) shows the microscopic PL image of structures and PL line scan obtained from confocal microscope using 410 nm diode laser. (d) Shows the variation of PL peak intensity and PL peak position across the structures. (e) Representative exciton PL spectra obtained from the central portion of the structure.

From Fig. 6, it is evident that the obtained microstructures show differences between the physical surface morphology to that of exciton PL morphology. While the SEM show fairly uniform structures, the exciton PL intensity mapping shows maximum at the center. Whereas, the PL peak position is constant at the centre but gradually red-shifted (about ~6 nm) at the edges. In our recent reports we have demonstrated the effect of layer crumpling and/or imperfect layered arrangement and/crumpling in thin films and crystal induces lowering of exciton energies [26]. The reason for more intense PL from the central portion of structure can be attributed to the long range order and perfect layering (less crumpling) arrangement. At the edges, slight non-uniform exciton energies could be due to layer crumpling/readjustment of the structures.

Further to give an insight and wide applicability of these thin film fabrication and to study the charge carrier transport for various optoelectronic device applications, the photocurrent measurements have been performed. A photodetector configuration has been realized by IO hybrid thin film on patterned transparent conducting substrate (ITO). Al-metal contacts are thermal vapor deposited on top of the film, where bottom ITO acts as anode and top Al-metal acts as cathode [Fig. 7(a)]. The photocurrent ON-OFF response for two different IO hybrid compositions y = 0.00 and y = 0.25 are recorded at 410 nm illumination (~109mW) [Fig. 7(b)]. Upon band edge illumination, both the compositions show potential photoresponse, having relatively faster response for Br contained IO hybrids. These preliminary studies can

#196165 - $15.00 USD Received 22 Aug 2013; revised 3 Nov 2013; accepted 6 Nov 2013; published 16 Dec 2013

be helpful in understanding the photocarrier transport phenomenon in such hybrids and support the applications where they acts as light harvesters, at the regime above bandgap as well as at exciton levels [21,31]. Therefore, the proposed mixed IO hybrid device quality thin films methodology may lead to better and efficient material for multifunctional applications, light emitting devices to solar cells and photodetectors. Moreover, the room-temperature low-cost processing of these semiconducting thin films of IO hybrids suggest the applicability of method for fabrication of thin film transistors (TFTs) [1] that require large area and the mechanical flexibility of plastic substrates.

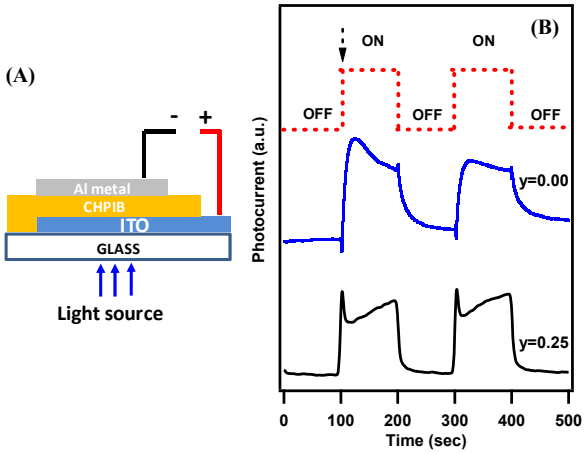

Fig. 7. (a) Schematic photodetector configuration showing the mixed IO hybrid as active material layer. (b) ON-OFF Photocurrent response characteristics recorded for $(C_6H_9C_2H_4NH_3)_2PbI_{4(1-y)}Br_{4y}$ at y = 0.00 and y = 0.25 under applied bias voltage of 1V and 410 nm illumination.

4. Conclusions

In summary, a unique cost-effective approach for fabrication of thin films of mixed inorganic-organic hybrid semiconductors $(C_6H_9C_2H_4NH_3)_2PbI_{4(1-y)}Br_{4y}$ (y = 0 to 1) has been successfully demonstrated. Room-temperature excitons from these mixed hybrids are being demonstrated from high quality IO hybrid thin films, those can be directly utilized in top-down technology and even can be carved into 3D shapes. This simple two-step methodology provides a potential niche for applications that require large areas, low cost, mechanical flexibility, or a combination of these factors. The experimental demonstration describes the utility of the approach for prototype fabrication of various optoelectronic devices like LEDs, photodetectors etc.

Acknowledgments

This work is funded by Department of Science & Technology (DST), India, British Council (UK-IERI), High-Impact Research scheme of IIT Delhi and Nano Research Facility (MCIT, Govt. of India). Authors are thankful to Prof. Jeremy Baumberg for his valuable suggestions and encouragement.

#196165 - $15.00 USD Received 22 Aug 2013; revised 3 Nov 2013; accepted 6 Nov 2013; published 16 Dec 2013